THE EFFECT OF CRYSTAL DEFECT DENSITY GRADIENTS ON RADIATION DAMAGE DEVELOPMENT AND ANNEAL.

A. García Celma , W. Soppe and H. Donker

ABSTRACT

Some modifications on the classical radiation damage simulation model developed by Jain and Lidiard are here presented. They simulate the effect on radiation damage of gradients of dislocation concentration, impurity concentrations, and radiation dose rate. With these modifications the heterogeneous colour distribution due to incipient colloid development observed in the microstructures of irradiated salt samples can be explained

1. INTRODUCTION

The primary defects formed during irradiation of NaCl are F– and H–centres. These complementary defect centres can, however, easily recombine, restoring the NaCl lattice. To produce permanent radiation damage these primary point defects have to be kept from recombining. In a perfect lattice, however, stabilizing point defects would be very difficult. Following Hobbs [1972], if dislocations are present, H–centres can be stabilized via a mechanism in which two H–centres "dig out" a NaCl ion pair from its regular position and form a Cl_2 molecule. The NaCl ion pair moves to the extra plain of the dislocation. Hobbs et al. [1973] also observed that during irradiation perfect edge dislocation loops in the [011] planes are formed. According to the mechanism described above, H–centres can be stabilized in places above and below (nearby and within the projection of) these dislocation loops. How the nucleation of these dislocation loops proceeds has however not been clarified. To circumvent this problem, in the theoretical models describing the radiation damage formation, it was either assumed that the dislocation loops already existed [Jain and Lidiard, 1977] or that other H–centre trapping

distortions (together with the H–centres) collapsed into dislocation loop structures [Seinen et al., 1992; Soppe, 1993]. Hobbs [1976] considered the distortion field around Na^+ lattice positions substitutionally occupied by divalent cation impurities as the most likely places for the nucleation of dislocation loops.

All models and theories assume the crystals to be homogenous entities since they disregard spatial distributions and perform calculations using only time–dependant concentration values. The general form of the mass balance of a given defect X, however, is:

$$\frac{\partial c_X}{\partial t} = Q_X^{source} - Q_X^{sink} + D_X \nabla^2 C_X \qquad (1)$$

In the theoretical models developed so far it is assumed that the salt is homogeneous and that there are no gradients in the concentrations of the various defects; i.e. the last term of (1) is zero. In the Jain–Lidiard model thus :

$$Q_F^{source} = K + 4\pi r_C C_C D_F c_F^{(e)} \qquad (2)$$

i.e. the production rate of F–centres (Q_F^{source}) is equal to their direct production rate (K) plus that of their evaporation from colloids ($4\pi r_c C_c D_F c_F^{(e)}$). On the other side, the F–centres concentration in solution diminishes (by an amount Q_F^{sink}) through recombination with H–centres, trapping at dislocation lines, recombination with Cl_2 molecules, and precipitation in the form of colloids. This is respectively represented by each term in (3)

$$Q_F^{sink} = K_2 c_F c_H + z_F \rho_d D_F c_F + \gamma D_F c_F c_A + 4\pi r_C C_C D_F c_F \qquad (3)$$

Similar expressions can be written for the H–centres, except that, for these centres, it is assumed that their precipitates in the form of Cl_2 are stable and therefore no H–centra evaporate from them. Taking into account this assumption the production rate of H centres is:

$$Q_H^{source} = K \qquad (4)$$

And the rate at which H–centres are taken out from the solution, which depends on similar processes as that of the F centres, is expressed as in (5)

$$Q_H^{sink} = K_2 c_F c_H + z_H \rho_d D_H c_H + 4\pi r_C C_C D_H c_H \qquad (5)$$

Then Jain and Lidiard define the rate of colloid production as the rate of sinking in of F centres :

$$Q_A^{source} = 4\pi r_C C_C D_F c_F \qquad (6)$$

And the rate of colloid annihilation as the evaporation rate of F centres from colloids plus the rate of H–centre recombination with colloids:

$$Q_A^{sink} = 4\pi r_C C_C D_F (c_F^{(e)} + c_H) \qquad (7)$$

As stated above, in the equations written by Jain and Lidiard it is assumed that the salt is homogeneous and that there is no variation in concentration of defects, nor gradients driving diffusion. However, something else than just random diffusion and random fixation of H–centres near randomly distributed impurities has to be envisaged if radiation damage has to be explained. Moreover randomness can never explain the heterogeneous colour distribution observed in irradiated samples.

In natural rock salts, intra en intercrystalline heterogeneities, all with extensions larger than some crystal lattice cells are always present and can be assumed to create gradients in defect concentrations which would drive diffusion in a preferent direction. Reinforcement of the concentration of a given colour centre (H– or F–centre) could then take place, but, since both (complementary) defects could be driven to diffuse in the same direction, annihilation could as

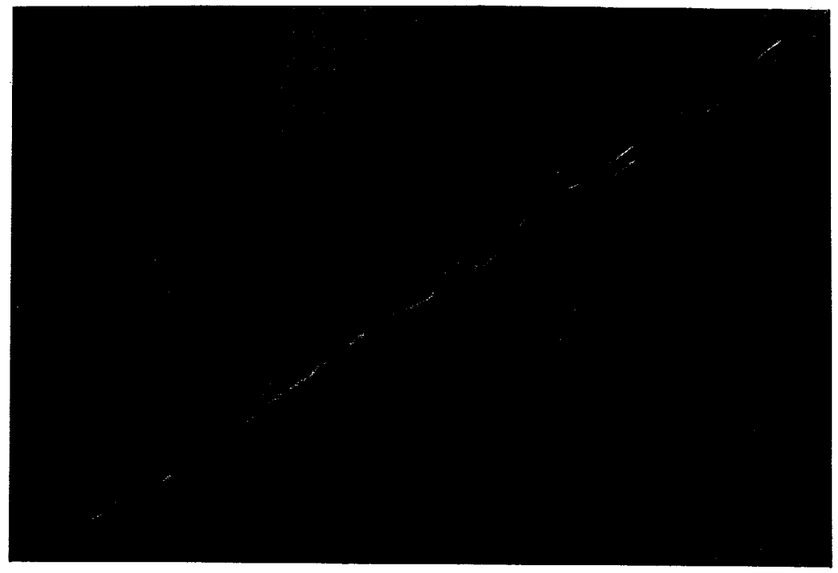

Figure 1 *Micrograph of a natural rock salt sample irradiated up to 2.6 MGy at 15 kGy/h and 100 °C. The black structure crossing the micrograph from top–right to bottom–left is a grain boundary void. Observe the colourless rim limited by the intense blue rim. The other colloid decorated structures are cellular patterns and incipient subgrain boundaries. Magnification 338 X.*

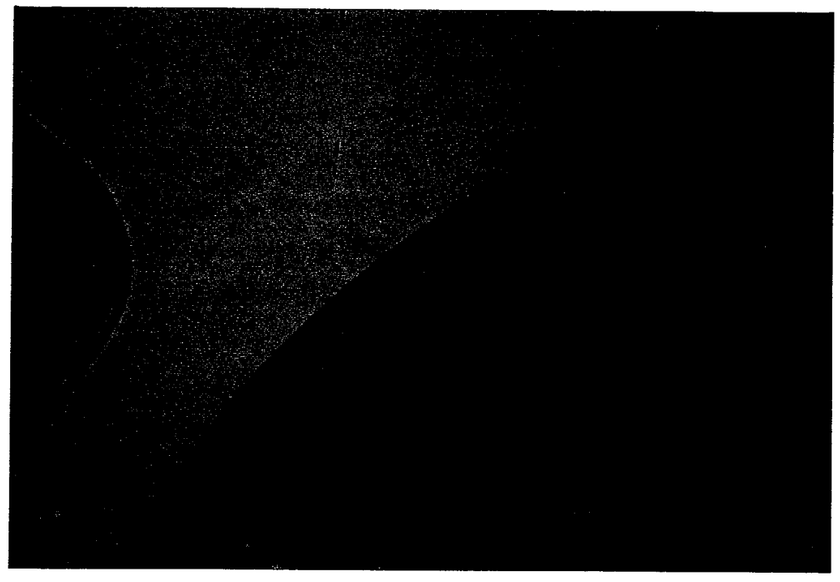

Figure 2 *Micrograph of a pure undeformed single crystal of NaCl irradiated up to 4 MGy at 15 kGy/h and 100 °C. Observe the dark colloid decorated, circular crystal outer surface. The outermost surface is too thin to be observed in this photograph but can be observed in Fig. 3. Magnification 34 X.*

well be the result. Both constructive and destructive results have been observed in the colour distribution. We try to obtain the "calculated" equivalents of the damage heterogeneity observed in the experiments through modelling the heterogeneities previous to the irradiation and the effect we believe they have on point defect dynamics. If the models reproduce the "heterogeneities" they would constitute a good test on our radiation damage development understanding.

As a basis we will use expression (1) for the mass balance of a defect X. Notice that in (1) a variation on the defect gradient ($D_x\nabla^2C_x$) is introduced which is never taken into account in the Jain–Lidiard model.

2. EXPERIMENTAL OBSERVATIONS

Intracrystalline distribution of damage is not homogeneous, but controlled by dislocation substructures. This is observed both on natural samples and on pure undeformed single crystals (Harshaw). It has been observed [Donker and García Celma, 1995] that rock salts do not contain more stored energy than Harshaw crystals irradiated simultaneously with them and under the same conditions. This contradiction with theoretical expectations is attributed, amongst other causes, to the fact that natural rock salts posses a more extense network of exterior crystal surfaces (sample boundaries, grain and subgrain boundaries, fractures) per volume of sample than the Harshaw crystals do, a higher density of exterior crystal surfaces would enhance creep due to the development of defect gradients in the crystals. The creep will take place associated with anneal even when the original heterogeneities will ease nucleation of radiation damage defects.

Incipient colloid development takes place near grain boundaries but at a distance from them. The grain boundary itself is colloid–free and at some distance to the exterior surface colloids appear constituting a dark blue line from which on and towards the centre of the crystal the blue colour becomes lighter (Fig. 1–3).

At a lower scale, the blue colour produced by the colloids is observed to display patterns which can be recognized as dislocation substructures. Most of these substructures were not present before irradiation and therefore are produced by the irradiation itself. The substructures grade from incipient slip bands (Fig. 3) , to well developed cross slip structures, subgrain

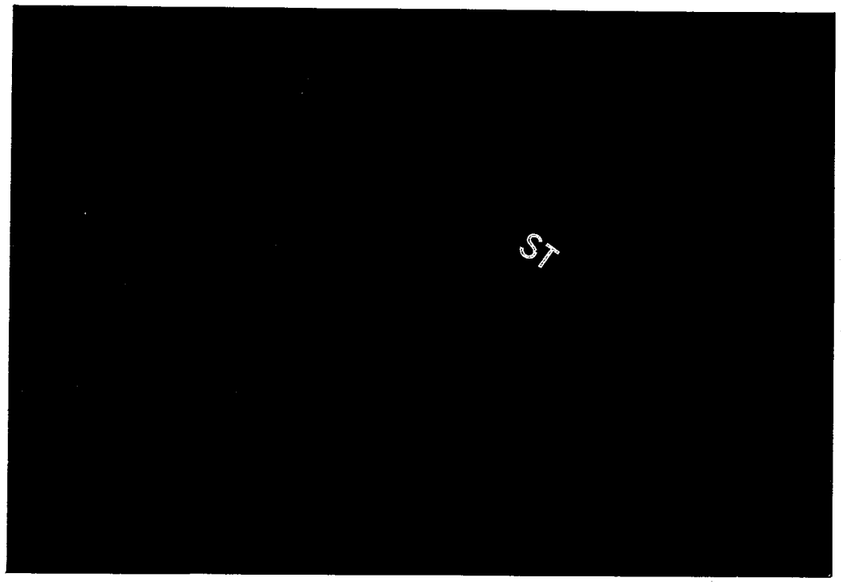

Figure 3 *Blow up of the dark rim of Fig.2. There is a colourless outer rim of the crystal which is seen as a less blue blurred rim at this magnification. The direction of incipient slip traces (ST) is indicated. The blue rim is made up of these incipient slip traces. Magnification 1343 X.*

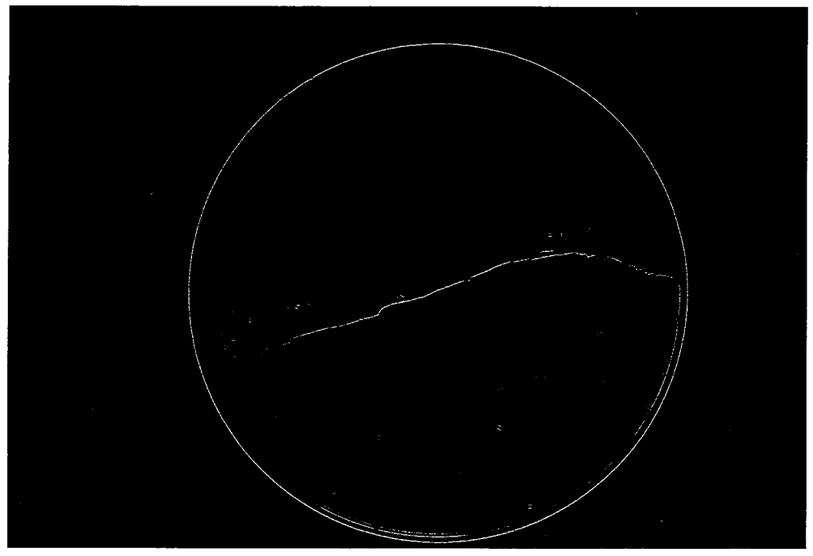

Figure 4 *Micrograph of a pure undeformed NaCl crystal irradiated up to 24 MGy at 15 kGy/h and 100 °C. The different darkness of parts of the crystal are a thin section preparation artifact. The colourless (white) lines network is a subgrain boundary network developed during irradiation. Magnification 4 X.*

Figure 5 *Micrograph of a natural rock salt sample irradiated up to 2.6 MGy at 15 kGy/h and 100 °C. Subgrain boundaries developing by climb of colloid decorated cross slip structures (cellular patterns), while near the polyhalite (P) boundary with the halite som of the subgrain boundaries already constitute a preferred diffusion path (incipient discolouration can be observed). Magnification 338 X.*

boundaries produced by dislocation climb processes (Fig. 4) and new grain boundaries of high surface equilibrium produced by polygonization due to further progression of this creep [García Celma and Donker, 1994]. Notice that since we observe them because they are blue, this means that when the dislocation migrate to constitute the various different arrangements the colloids are either destroyed and re–nucleated or migrate together with the creep structures.

Those substructures which are material discontinuities are observed as a white rim limited by a blue rim with the same structure as observed for incipient colloid development (see Fig. 5,6). If the material discontinueties were already present in the sample at the beginning of the irradiation it can be assumed that colloids did not develop at the exterior surface as is the case with Harshaw single crystals. However, if they are produced by creep during irradiation by dislocation wall development (e.g. subgrain boundaries) (Fig. 4) it has to be assumed that bleaching took place since dislocation lines are first blue. An extreme example of this colloid distribution was obtained in the Brine Migration Test [Gies et al.,1994] (see Fig. 7).

3. HETEROGENEOUS DISLOCATION DISTRIBUTION

Natural rocks compact by adaption to the strain (deformation) produced by the overlying pack of rocks. When stress results in plastic deformation, dislocations and their arrangements are the lattice expression of the strain undergone by the rock. Dislocations in deformed materials mostly display a core–mantle distribution. This means that the mantles of the crystals protect their inner parts (the cores) from the action of externally applied deformation through plastically adapting themselves to the deformation, and thus accumulate dislocations.

Therefore, the dislocation density at the mantle is many times bigger than at the core of any crystal. Lets thus assume a spherical grain with radius R where the distribution of the dislocations is described by:

$$\rho_d(r,t) = \rho_d e^{-\kappa(R-r)} \qquad (8)$$

Since we may assume that the concentration of the H centres is steady ($\delta c_H/\delta t = 0$), the

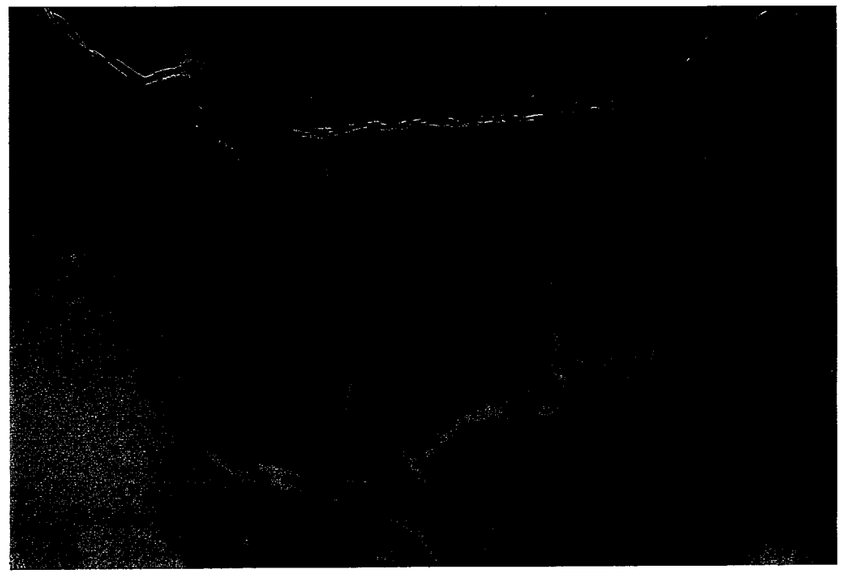

Figure 6 *Micrograph of a natural rock salt sample irradiated up to 4 MGy at 15 kGy/h and 100 °C. Well developed subgrain boundaries ending at a grain boundary, all bleached by preferred diffusion of radiation damage defects towards the grain boundary void. Magnification 338 X.*

Figure 7 *Micrograph of a natural rock salt sample from the Brine Migration Test (in situ irradiation experiment at the Asse Mine). Observe the very exaggerated white (colourless) rims near the grain boundaries and the blue rims fading towards the grain cores. Magnification 7 X.*

contribution of the diffusion of H centres is easy to determine if we also assume that it is a second order effect. We can then write:

$$\nabla^2 c_H = \nabla^2\left(\frac{K}{K_2 c_F + z_H \rho_D D_H + D_H 4\pi r_C C_C}\right) = \frac{1}{r^2}\frac{\partial}{\partial r}\left(r^2 \frac{\partial}{\partial r}\right)\frac{K}{A + B\rho_d(r,t)} \qquad (9)$$

where $A = K_2 c_F + 4\pi r_c C_c D_H$, and $B = z_H D_H$, equation (9) then gives:

$$\nabla^2 c_H = -\frac{\kappa K B \rho_d(r,t)}{(A + B\rho_d(r,t))^2}\left[\frac{2}{r} + \kappa - \frac{2\kappa B \rho_d(r,t)}{A + B\rho_d(r,t)}\right] \qquad (10)$$

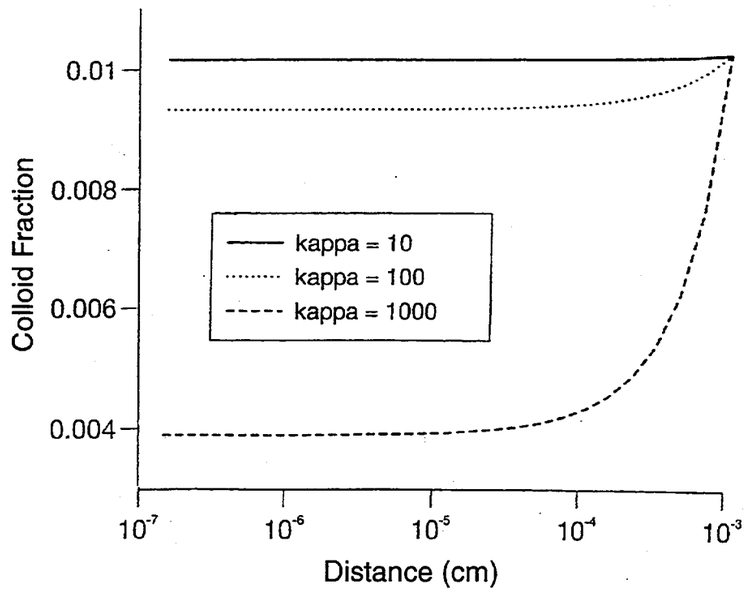

Figure 8 *Calculated colloid fraction as a function of distance from the grain core for a spherical grain of radius 10^{-3} cm, assuming a heterogeneous dislocation distribution (see text). Dose rate 100 kGy/h, total dose 833 MGy*

The diffusion term for the F–centres is more difficult to consider because we do not have any analytical expression for their concentration as a function of crystal radius and time. We have tried some approximations but they all lead to difficulties in integrating $\partial c_F/\partial t$. If the diffusion term for the F–centres is not considered and the heterogeneities are only expressed using (8), the differential equations for c_F and c_H could be integrated. The results of the model for three different values of κ are represented in Fig. 8. The value assumed for the dose rate K was 100 kGy/h, and the total dose 833 MGy. It can be seen that in these simulations the colloid fraction follows more or less the behaviour of the dislocation line density: a maximum concentration at the grain boundary and an exponential decrease in the direction of the grain core.

4. THE EFFECT OF THE GRAIN BOUNDARY

In the previous chapter we have shown that we can explain that regions of the crystals where many dislocations are present develop more radiation damage than regions with lower dislocation densities. In natural rock salts the highest dislocation densities are expected at the grain boundaries. However, the first place where colloids develop in natural samples is not at but near the grain boundaries and in Harshaw crystals near the crystal boundary. The crystal/grain boundaries themselves tend to be devoid of colloids while the colloids are observed in the optical microscope as accumulating at a given distance between 2 and 7 microns of the free surface of the crystal/grain. Towards the crystal/grain interior the colloid concentration gradually diminishes. See the micrographs in Fig. 1–3.

One of the most important differences with a perfect crystal (as assumed in the models) displayed by the crystals used in our experiments is that the real crystals are finite and that they have exterior surfaces. The exterior surfaces can be described as an accumulation of dislocations. To simulate the grain boundary we considered that there are three dislocation lines per unit cell at the exterior surface of the grain, and that the dislocation density is many times bigger at the mantle than at the core of an halite crystal. We have approximated this by the following expression:

$$\rho = \rho_1 e^{-\kappa(R - r)} + \rho_d \qquad \textbf{(11)}$$

in which r is the distance from the grain boundary, ρ_1 is the dislocation density at the surface and ρ_d is the dislocation density in the bulk of the crystal. Notice that this expression is very similar to Eq. (8). The main difference, however is that the dislocation density at the surface is now many orders of magnitude higher than in (8)

Using Eq. (11) the Jain–Lidiard model gives the colloidal distribution displayed in Fig. 9. In Fig. 9 the dose rate K= 100 kGy/h ; total dose simulated was 833 MGy, $\kappa = 10^4$ cm^{-1}, and $\rho_1 = 10^{12}$ cm^{-2}. From Fig. 9 it can be observed that the colloid distribution predicted by the model agrees with the experimental observations, i.e. the model predicts that a maximum colloid concentration will occur at a few microns from the surface of the crystal/grain and that the surface itself will be devoid of colloids.

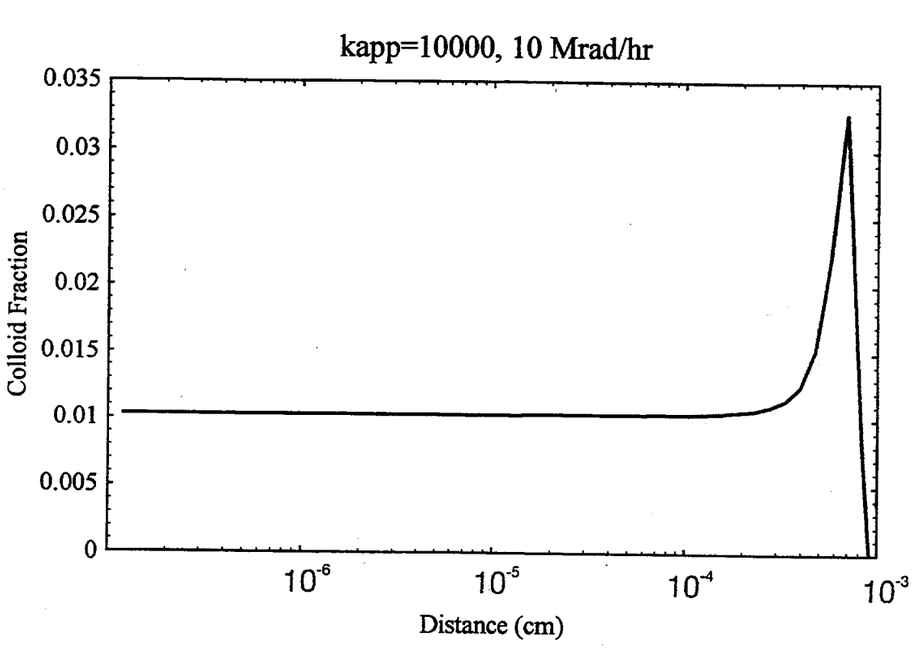

Figure 9 *Calculated colloid fraction as a function of distance from the grain core for a spherical grain of radius 10^{-3} cm, assuming a dislocation distribution according to Eq. 11 (see text). Dose rate 100 kGy/h, total dose 833 MGy, $\rho_1 = 10^{12}$ cm^{-2} and $\kappa = 10^4$ cm^{-1}.*

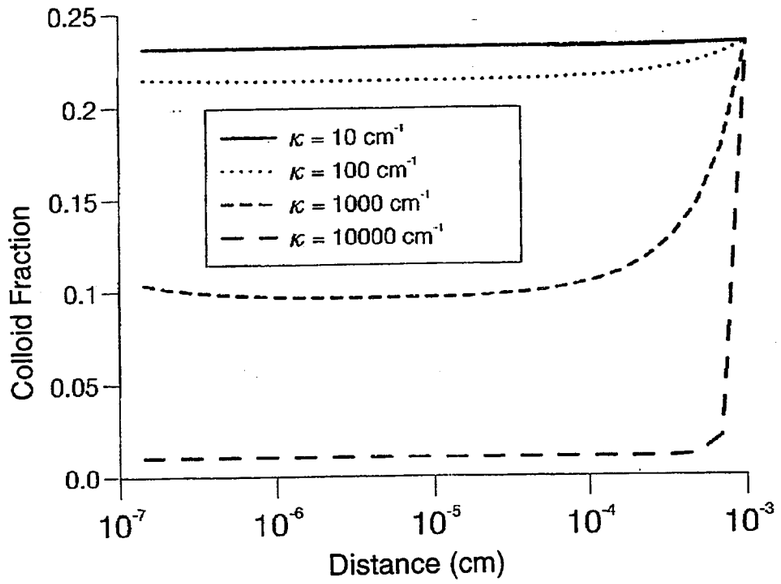

Figure 10 *Calculated colloid fraction as a function of distance from the grain core for a spherical grain of radius 10^{-3} cm, assuming a heterogeneous impurity distribution (see text). Dose rate 100 kGy/h, total dose 833 MGy.*

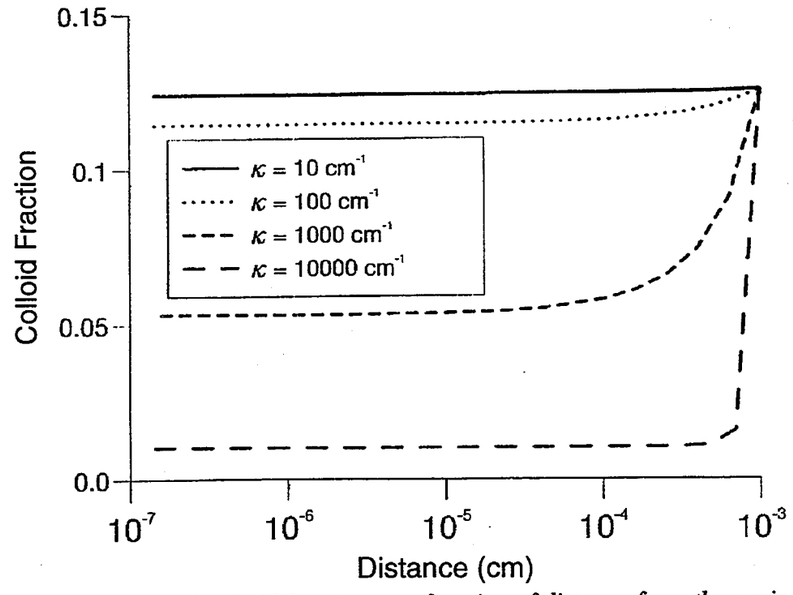

Figure 11 *Calculated colloid fraction as a function of distance from the grain core for a spherical grain of radius 10^{-3} cm, assuming a heterogeneous impurity distribution but disregarding the effect of diffusion (see text). Dose rate 100 kGy/h, total dose 833 MGy.*

$\kappa=10^3$ cm^{-1}, but further inspection of them learns that all curves have this same behaviour. The cause of this is that $\nabla^2 c_H$ is divergent for $r = 0$ because $c_S(0)$ is not equal to zero.

In Fig. 11 the results of simulations only differing from the previous in that they disregard the effect of diffusion have been presented. Two important differences with Fig. 10 can be observed in Fig. 11, first the colloidal fraction is systematically much lower (about a factor 2) than in Fig. 10; and second the U–form character of the curves has disappeared. We can see that the diffusion–term in this case is very important and cannot be disregarded.

6. THE REPOSITORY.

On top of all the previously considered heterogeneities, there is as well an important gradient at the scale of a repository, e.g. the gradient resulting from the absorption of the gamma radiation by salt near the containers. This can be modelled as a gradient in the dose rate.
At the scale of the salt grains the dose rate gradient as a consequence of the sensitivity to "stopping rate" can be disregarded. However the question is whether the gradient which in a repository would develop radially away from the containers would significantly contribute to the diffusion . It is easy to observe that this is not the case. Lets assume that the dose rate can be described with:

$$K(d) = K_0 e^{-\kappa d} \tag{16}$$

where d is the distance to the container. This leads to:

$$\nabla^2 c_F \propto \frac{1}{4}\kappa^2 c_F \quad \text{and} \qquad \nabla^2 c_H \propto \kappa^2 c_H \tag{17}$$

Now κ is of the order of magnitude of 1 cm^{-1} and $D_F c_F$ and $D_H c_H$ lie between 10^{-18} and 10^{-14} cm^2/s for $T \approx 100$ °C. If we now know that the dose rate of 10 kGy/h corresponds with

$$c_S(r) = c_{S,0}\, e^{-\kappa(R-r)} \tag{12}$$

then, the zero order steady state equation for the H–centres is :

$$c_H = \frac{K}{K_2 c_F + z_H \rho_D D_H + D_H 4\pi r_C c_C + K_H c_S(r)} \tag{13}$$

What gives (see equation (10)):

$$\nabla^2 c_H = -\frac{\kappa K D c_S(r)}{(C + D c_S(r))^2}\left[\frac{2}{r} + \kappa - \frac{2\kappa D c_S(r)}{C + D c_S(r)}\right] \tag{14}$$

where $C = K_2 c_F + z_H \rho_d D_H + D_H 4\ \pi r_C C_C$. , and : $D = K_H$.

The first order steady state equation for the H–centres then becomes:

$$c_H = \frac{K + D_H \nabla^2 c_H}{K_2 c_F + z_H \rho_D D_H + D_H 4\pi r_C c_C + K_H c_S(r)} \tag{15}$$

We were able to solve the "ordinary" equations for the F–centres (as determined by equations (2) and (3)), and for the colloids (as determined by equations (5) and (6)) in combination with these last expressed boundary conditions. The results for 4 values of κ are given in Fig. 10 for $c_{S,0} = 10^{-6}$, K equal to 100 kGy/h, and a total dose of 833 MGy. Firstly we can see that the colloidal fractions are in general higher than in the case considered for the dislocations, this is the effect of the impurities in general. For $\kappa = 10^4$ cm^{-1}, c_S(r) is almost zero for $r = 0$ and we observe that the colloid fraction is also the same as that found for the dislocations. Moreover, it can be seen that the curves have an U shape (This can best be seen for

5. HETEROGENEOUS IMPURITY DISTRIBUTION

During crystal growth, lattice impurities tend to be preferently segregated towards the crystal exterior surfaces. Some crystals incorporate progressively higher concentrations of lattice impurities as they become bigger, and some times even stop growing due to "poisoning" of the growing surfaces by the impurities Moreover, in a closed system, a crystal growing from solution is bound to incorporate more and more impurities while growing (due to the changes in the solution concentration) until the exterior surface is "poisoned" and growth stops. In autigenic crystals, therefore it is logical to expect higher impurity concentrations near the crystal boundaries.

The impurity distribution in secondary crystals, which contrary to the autigenic have undergone some degree of recrystallization, can partially have controlled the mechanical behaviour of the crystal during the processes subsequent to crystallization. On the other side, the distribution of the impurities after a deformation process will be affected by deformation, e.g. impurities will partially redistribute themselves by diffusion towards the distended parts of the lattice which are dislocations and their arrangements.

Anyway, in rock forming minerals, impurities and dislocations have a tendency to fall near (and within) each other's sphere of influence, and to display gradients at grain and subgrain level.

Jain en Lidiard did not consider the effects of lattice impurities on the production of radiation damage. It can be assumed that certain impurities act as trapping environments for H centres and thus provoke an enhanced colloid growth. This assumption leads to an extra (negative) term in equation (5) : $K_H c_S c_H$ where c_S is the concentration of the impurities and K_H a reaction constant.

Lets assume, to ease our work, that the impurity concentration is stable and nonsaturable, we will therefore not consider the development of H–dimers.

Assuming that the space dependence for the impurities in an spherical grain is equal to that assumed for the dislocations so that:

$K = 1.667 \times 10^{-8}\ s^{-1}$ we can see that the contribution to diffusion is only relevant for very low dose rates (or for very high temperatures). Under these situations, indeed, no colloid growth can take place, and thus we could conclude that in general the diffusion contribution as consequence of a gradient in dose rate K can be disregarded as compared with the effect of K itself.

7. CONCLUSIONS

With the implemented modifications the Jain–Lidiard model is capable of reproducing the observed microstructures for incipient colloid development. However, since the dynamics of the dislocations and impurities have not been modelled we are not yet able to explain why and how the colour distribution follows the creep structures.

8. REFERENCES

H. DONKER and A. GARCÍA CELMA, 1995: *"Stored Energy in Irradiated Natural Rock Salt as Compared to Synthetic Halite of Different Characteristics"*, article 17 of this volume.

A. GARCÍA CELMA and H. DONKER, 1994: *"Radiation–Induced Creep of Confined NaCl"*, Rad. Eff. Def. Solids **132**, 223–247.

H. GIES, A. GARCÍA CELMA, J.B.M. DE HAAS, L. PEDERSON, T. ROTHFUCHS, 1994: *"Radiation Defects and Energy Storage in Natural Polycrystalline Rock Salt. Results of an In–situ Test in the Permian Rock Salt of the Asse"*, Mat.Res. Soc. Symp. Proc. **333**, 219–226

L.W. HOBBS, 1972: *"Transmission Electron Microscopy of Extended Defects in Alkali Halide Crystals"*, in "Surface and Defect Properties of Solids", Vol. 4, Specialst Periodical Reports, Ed. J.M. Thomas and M.W. Roberts (The Chemical Society, London), p. 152 – 250

L.W. HOBBS, 1976: *"Point Defect Stabilization in Ionic Crystals at High Defect Concentrations"*, J. Physique **37**, C7, 3–26

L.W. HOBBS, A.E. HUGHES and D. POOLEY, 1973: *"A Study of Interstitial Clusters in Irradiated Alkali Halides using Direct Electron Microscopy"*, Proc. R. Soc. Lond. **A332,** 167–185.

U. JAIN and A.B. LIDIARD, 1977: *"The Growth of Colloidal Centres in Irradiated Alkali Halides"*, Phil. Mag. **35**, 245–259.

J. SEINEN, J.C. GROOTE, J.R.W. WEERKAMP and H.W. DEN HARTOG, 1992: *"Radiation Damage in NaCl: General Model of Nucleation and Aggregation Processes in Doped NaCl"*, Rad. Eff. Def. Solids **124**, 325–339.

W.J. SOPPE, 1993: *"Computer Simulation of Radiation Damage in NaCl by using a Kinetic Rate Reaction Model"*, J. Phys.: Condensed Matter **5**, 3519–3540.